

Hall hole mobility in boron-doped homoepitaxial diamond

J. Pernot,* P. N. Volpe, F. Omnès, and P. Muret

Institut NEEL, CNRS and Université Joseph Fourier, BP 166, 38042 Grenoble Cedex 9, France

V. Mortet and K. Haenen

*Institute for Materials Research (IMO), Hasselt University, Wetenschapspark 1, B-3590 Diepenbeek, Belgium
and Division IMOMEK, IMEC vzw, Wetenschapspark 1, B-3590 Diepenbeek, Belgium*

T. Teraji

National Institute for Materials Science, 1-1 Namiki, Tsukuba, Ibaraki 305-0044, Japan

(Received 14 December 2009; published 7 May 2010)

Hall hole mobility of boron-doped homoepitaxial (100) diamond samples has been investigated in the temperature range of 100–900 K, both experimentally and theoretically. The temperature dependence of the mobility measured in high-quality and low boron-doped materials was compared with theoretical calculations to determine the phonon-hole coupling constants (deformation potential for acoustic phonons and coupling constant for optical phonons). The maximum hole mobility is found to be close to 2000 cm²/Vs at room temperature. For boron-doped material, the hole scattering by neutral boron atoms is shown to be important in diamond due to the high ionization energy of the boron acceptor. The doping dependence of the Hall hole mobility is established for boron-doping levels ranging between 10¹⁴ and 10²⁰ cm⁻³ at 300 and 500 K. The physical reasons which make diamond a semiconductor with a higher mobility than other semiconductors of column IV are discussed.

DOI: [10.1103/PhysRevB.81.205203](https://doi.org/10.1103/PhysRevB.81.205203)

PACS number(s): 72.20.Fr, 72.80.Cw, 72.20.Dp

I. INTRODUCTION

Diamond is a fascinating material due to its exceptional physical properties such as wide band gap, high breakdown voltage, high thermal conductivity, and high carrier mobility. For semiconductor physics, this is a very attractive material because the physical concepts developed for narrower band-gap semiconductors can be investigated in the case of extreme limits (high phonon energy, high ionization energy of dopants, small Bohr radius of electron, or hole bounded to impurities, etc.). One of the most impressive properties of diamond is its high carrier mobility and particularly for holes. Recently, Isberg *et al.*¹ reported very high values of mobility using a time-of-flight technique. Even if these very high values of mobility has never been reproduced using the same material,² diamond hole mobility is clearly higher than in other neighbor semiconductors as Si or 4H-SiC. A detailed description of the doping dependence of the mobility in the case of *n*-type doped material has been recently reported^{3,4} but a full picture of the mobility properties in case of *p*-type is still lacking. *p*-type doping is now well mastered. Boron is known as the most attractive single-electron acceptor impurity for diamond ($E_i \approx 0.37$ eV) and a gradual change from a semiconductor to a metal and eventually to a superconductor is observed as the boron doping level increases above 5×10^{20} cm⁻³.^{5,6} Concerning the mobility in *p*-type doped diamond, even if the temperature dependence of the mobility and carrier density of homoepitaxial boron-doped diamond have been studied by a lot of groups,^{7–15} only one of these works reports a detailed description of the scattering mechanisms responsible of the mobility limitation.¹¹ Unfortunately, in this latter work, one scattering mechanism (neutral impurity scattering) is not taken into account leading to (i) an unexpected difference between the compensation centers

density determined from the mobility analysis and the density analysis for highly doped samples and (ii) an unexpected variation in the acoustical deformation potential with the doping level.

In this work, the Hall mobility of homoepitaxial boron-doped diamond is investigated in a large temperature range and large doping range for samples grown by different groups. It is shown that for low boron-doping level, the low-temperature mobility is governed by ionized impurity scattering (mainly due to compensation) and the high-temperature mobility by phonon scattering (acoustical or optical with an intraband or interband process). For strong boron-doping levels, the low-temperature mobility is completely limited by the neutral impurity scattering (neutral boron atoms), making the highest room-temperature mobility dependent of the doping level. The paper is organized as follow: in Sec. II, we review the theoretical background concerning the method of mobility analysis. In Sec. III, the intrinsic phonon parameters of *p*-type diamond are deduced from mobility temperature dependence fitting of high-quality diamond samples. Then, the model is used to describe the boron-doping dependence of the Hall hole mobility in {100} homoepitaxial diamond samples at 300 and 500 K. Finally, the physical reasons which lead to a larger mobility in diamond than in Si and 4H-SiC are given. The paper is concluded by a brief summary.

II. THEORETICAL BACKGROUND

In this section we review the background considerations concerning the hole effective masses, the neutrality equation, the scattering modes, the Hall coefficient, and the mobility. For each topic we quote the relevant literature and material

parameters used in the subsequent calculations. The transport analysis is carried out using a three-band transport model at low field, similar to the one presented by Lee and Look¹⁶ for GaAs or Pernot *et al.*¹⁷ for 4H-SiC in the case of two bands. R_{Hi} and σ_i ($i=lh, hh, so$) in which lh, hh, and so refer to the light hole (lh), heavy hole (hh), and spin-orbit (so) hole, respectively, are calculated separately for each band and combined using classical multiband equations.

A. Band structure

Few experimental and theoretical descriptions of the dispersion of the topmost valence bands in diamond have been given by several groups (see references in Ref. 18). They deduced Luttinger parameters but in disagreements between each others. Willatzen *et al.*¹⁸ have done *ab initio* calculations using linear muffin-tin-orbital method in local-density approximation which is well known to be one of the most realistic method to determine the band structure, and so the effective masses, in semiconductors. They show that the three uppermost valence bands have their maximum localized at the Γ point of the Brillouin zone. The two upper bands are degenerated at the Γ point and energetically positioned at a higher energy than the third hole band by the spin-orbit coupling (13 meV). This spin-orbit value is close to the one found experimentally of 6 meV.¹⁹ In this work and in order to simplify the analysis, the small energy gap between the two uppermost bands (named in this work lh and hh) and the third one (named in this work so) is not taken into account and the three bands are considered as degenerated in the Γ point of the Brillouin zone. The three valence bands are considered to be parabolic with representative effective masses of Ref 18: $m_{hh}^{*100}=0.427 m_0$, $m_{hh}^{*110}=0.69 m_0$ for the heavy holes, $m_{lh}^{*100}=0.366 m_0$, $m_{lh}^{*110}=0.276 m_0$ for the light holes, and $m_{so}^*=0.394 m_0$ for the spin-orbit holes. The corresponding values for the density of state mass are $m_{hh}^*=[(m_{hh}^{*110})^2 m_{hh}^{*100}]^{1/3}=0.588 m_0$ and $m_{lh}^*=[(m_{lh}^{*110})^2 m_{lh}^{*100}]^{1/3}=0.303 m_0$. Finally, to compute the position of the Fermi level for a given free hole population, we get the total density-of-state mass $m^*=(m_{lh}^{*3/2}+m_{hh}^{*3/2}+m_{so}^{*3/2})^{2/3}=0.908 m_0$.

B. Hole scattering mechanisms

Four hole scattering mechanisms have been considered: ionized impurity (ii) scattering, neutral impurity (ni) scattering, acoustic phonon (ac) scattering, and nonpolar optical phonon (op) scattering. The relaxation times corresponding to the different scattering mechanisms are described below.

1. Ionized impurities

The scattering by ii is described in Ref. 20 for the case of electrons in the conduction band. We simply adjust the relaxation time to the case of the valence band by taking into account the p -type symmetry of wave functions in place of the s -type wave functions, as discussed elsewhere.²¹ As a consequence, with respect to the conduction band, the relaxation time of the valence band is multiplied by a factor of 1.5. The inverse relaxation time is then (MKS units)

$$\frac{1}{\tau_{ii}} = \frac{2}{3} \frac{N_I e^4}{16\sqrt{2}\pi(\epsilon_s \epsilon_0)^2 m_i^{*1/2}} F_{ij} \mathcal{E}^{-3/2}, \quad (1)$$

where i runs over light holes, heavy holes, and holes of the spin-orbit band, $N_I=p+2N_D$ is the density of charged ions in the p -type material, p is the total hole density, ϵ_s is the static dielectric constant, $\epsilon_0=10^7/(4\pi c^2)$ F m⁻¹ is the vacuum permittivity, c is the light velocity in vacuum, and

$$F_{ij} = \ln(\xi + 1) - \frac{\xi}{\xi + 1}, \quad (2)$$

where $\xi=(2k\lambda)^2$, in which λ is the screening length and k is the electron wave vector. The latter can be calculated for arbitrary degeneracy, but, for a nondegenerate case is

$$\frac{1}{\lambda^2} = \frac{e^2}{\epsilon_s \epsilon_0 k_B T} \left[p + \frac{(N_A - N_D - p)(p + N_D)}{N_A} \right], \quad (3)$$

where N_A and N_D are the total densities of acceptors and donors, respectively. For the static dielectric constant $\epsilon_s=5.7$ has been used. This assumption is reliable in our case since the doping level of the samples investigated in this work is below 1.7×10^{19} cm⁻³ which is more than one order of magnitude below the density of the metallic transition at 5×10^{20} cm⁻³ corresponding to the degenerate case.⁵

2. Neutral impurities

The scattering by ni is very important in n -type diamond.^{3,4} This is because the donor binding energy is so large that, at low temperatures, the majority of impurities is neutral, but not so large, that the Bohr radius of the bound electron allows scattering of the electrons in the conduction band. In the case of acceptor species, it is shown in this work that this is the main scattering mechanism for the highly doped sample at low temperature. The relaxation time can be calculated with the simple approach of Erginsoy,²² in analogy with atomic physics. We use the more complete approach of Meyer and Bartoli²³ (cf. also Blagosklonskaya *et al.*²⁴ and McGill and Baron²⁵). The relaxation time, as deduced from Ref. 23, is

$$\frac{1}{\tau_{ni}} = \frac{A(\omega) N_n 4\pi\epsilon_s \epsilon_0 \hbar^3}{m^{*2} q^2}, \quad (4)$$

where $N_n=N_A-N_D-p$ is the number of neutral impurities and

$$A(\omega) = \frac{35.2 (1 + e^{-50\omega})(1 + 80.6\omega + 23.7\omega^2)}{\omega^{1/2} (1 + 41.3\omega + 133\omega^2)} \times \left[\frac{1}{\omega} \ln(1 + \omega) - \frac{1 + \frac{1}{2}\omega - \frac{1}{6}\omega^2}{1 + \omega^3} \right]. \quad (5)$$

Here $\omega=\epsilon/E_B$ in which E_B is the boron acceptor binding energy taken at 370 meV. We must keep in mind that this procedure is inexact because it is clear that deep acceptor such as boron in diamond is not purely hydrogenic. Although the energetic positions of excited states of boron are also quite well described by using a hydrogenlike model.²⁶ The

approach of Meyer and Bartoli²³ has been demonstrated to be more reliable than the simple approach of Erginsoy²² [see, for example, in the case of isotopically engineered Ge (Ref. 27)].

3. Acoustic phonons, intraband, and interband processes

The relaxation time due to the scattering by ac is reviewed, for instance, in the work of Ref. 28. Because the acoustic phonons have a small, but finite, wave vector and because the valence band is (almost) degenerate at $k=0$ both intraband and interband processes occur. The total density of states, into which a free hole can be scattered, is then proportional to $(m_{\text{lh}}^{*3/2} + m_{\text{hh}}^{*3/2} + m_{\text{so}}^{*3/2})$ which, introduced into the relaxation time,²⁹ gives

$$\frac{1}{\tau_{\text{ac}}} = \frac{\sqrt{2}(m_{\text{lh}}^{*3/2} + m_{\text{hh}}^{*3/2} + m_{\text{so}}^{*3/2})C_a^2 k_B T}{\pi \hbar^4 \rho v_{\parallel}^2} \varepsilon^{1/2} \quad (6)$$

$\rho=3515 \text{ kg m}^{-3}$ is the crystal mass density, $v_{\parallel}=17536$ is the velocity of longitudinal acoustic phonons, and C_a is the acoustic deformation potential. C_a was treated as an adjustable parameter.

4. Nonpolar optical phonons, intraband, and interband processes

The scattering due to op is either intraband or interband. In our calculation, we use the combined relaxation time of intraband and interband scatterings³⁰

$$\begin{aligned} \frac{1}{\tau_{\text{op}}} &= \frac{1}{\tau_{\text{op},ii}} + \frac{1}{\tau_{\text{op},ij}} \\ &= \frac{(D_{ii} + D_{ij})^2 (m_{\text{hh}}^{3/2} + m_{\text{lh}}^{3/2} + m_{\text{so}}^{3/2})}{\sqrt{2} \pi \rho \hbar^3 \omega_0} \\ &\quad \times \{N(\omega_0)(\varepsilon + \hbar \omega_0)^{1/2} + [N(\omega_0) + 1](\varepsilon - \hbar \omega_0)^{1/2}\}, \end{aligned} \quad (7)$$

where $N(\omega_0)=1/\{\exp[\hbar \omega_0/(k_B T)]-1\}$ is the phonon occupation factor and $\tau_{\text{op},ii}$ and $\tau_{\text{op},ij}$ are the intraband (*ii*) and interband (*ij*) relaxation times due to nonpolar optical phonons. The phonon emission terms $N(\omega_0)+1$ contribute only for $\varepsilon \geq \hbar \omega_0$, otherwise they vanish. For the optical phonon energy at small values of the phonon wave vector we used a representative phonon energy $\hbar \omega_0=165 \text{ meV}$. This phonon energy corresponds to an average energy of the optical phonon modes at the Γ point of the Brillouin zone.³¹ In this approach the summation over all possible initial and final states is represented by an effective coupling constant $(D_{ii}+D_{ij})$ which takes into account the intraband scattering (D_{ii}) and the interband scattering (D_{ij}). It should be emphasized that these coupling constants have a rather “effective” meaning since we cannot distinguish D_{ii} and D_{ij} individually by comparison with experiments. So we have determined (as was the case for the deformation potential of the acoustic phonon mode), the sum of the coupling constants due to intraband and interband scatterings.

C. Hall mobility

The total relaxation time is obtained from the Mathiessen rule

$$\frac{1}{\tau} = \sum_n \frac{1}{\tau_n} \quad (8)$$

in which τ_n is the relaxation time assigned to scattering mechanism n . To take into account the inelasticity of the op mode, the procedure introduced by Farvacque³² is used. The average value of the relaxation time $\bar{\tau}$ and the ohmic mobility $\mu=e\bar{\tau}/m^*$ are then directly computed.

D. Hall scattering factor

To compare with experimental data, one needs to introduce the combined Hall scattering factor r_H . It depends on (i) the scattering mechanisms, (ii) the anisotropy of the scattering mechanisms, and (iii) the anisotropy of the valence-band energy surface (for a review, see Wiley²¹). In the three band approach, it can be written³³

$$r_H = (p_{\text{hh}} + p_{\text{lh}} + p_{\text{so}}) \frac{r_{\text{hh}} \mu_{\text{hh}}^2 p_{\text{hh}} + r_{\text{lh}} \mu_{\text{lh}}^2 p_{\text{lh}} + r_{\text{so}} \mu_{\text{so}}^2 p_{\text{so}}}{(\mu_{\text{hh}} p_{\text{hh}} + \mu_{\text{lh}} p_{\text{lh}} + \mu_{\text{so}} p_{\text{so}})^2}. \quad (9)$$

Reggiani *et al.*³⁴ have calculated the Hall scattering factor in the case of p -type diamond within the relaxation time approximation with the different sets of inverse valence-band parameters available in the literature. They obtained two set of values of r_H , one which gives r_H systematically larger than one and one which gives r_H systematically smaller than one. By comparison with the ratio between Hall and drift mobility, they deduced that the later is the correct one. Unfortunately, Szmulowicz for Si and Ge (Ref. 35) as well as Look *et al.*³³ for GaAs have shown that the relaxation-time approximation is not best suited to calculate the Hall scattering factor in p -type material. However, the fact that the drift mobility is generally larger than the Hall mobility when intrinsic scattering occurs (such as phonon scatterings) seems to show that the Hall scattering factor is less than unity. Since we are not able to describe correctly the Hall scattering factor and its temperature dependence, we approximate r_H by unity in this work.

The equation used to compare with experimental values of the Hall mobility σR_H is then

$$\mu_H = \frac{p_{\text{hh}} \mu_{\text{hh}} + p_{\text{lh}} \mu_{\text{lh}} + p_{\text{so}} \mu_{\text{so}}}{p_{\text{hh}} + p_{\text{lh}} + p_{\text{so}}}. \quad (10)$$

III. RESULTS

A. Mobility in low boron-doped diamond—temperature dependence

In Sec. II B, some intrinsic mobility parameters appear. They are the acoustic deformation potential (C_a) for the ac mode and the effective coupling constant $(D_{ii}+D_{ij})$ for the op mode. In order to determine these intrinsic parameters of diamond, we compare the calculated mobility for high-quality low boron-doped diamond which have been selected in the literature.^{8,12,13,15} The sample with the highest mobility in the literature has been measured in the high-temperature range (300–700 K) to complete the existing data.¹³ The temperature dependence of the Hall mobility is shown on Fig. 1

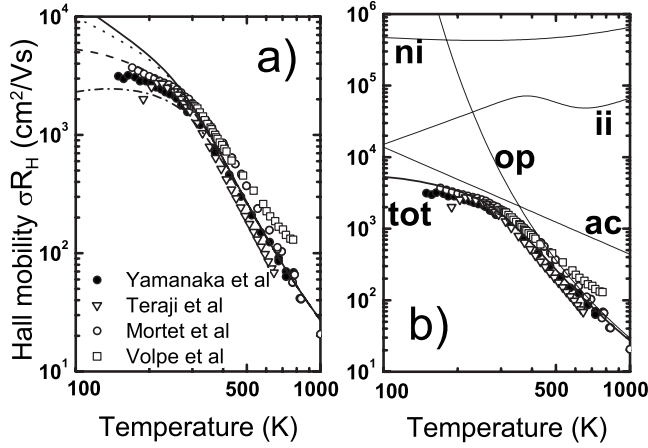


FIG. 1. Temperature dependence of the Hall mobility (σR_H). Experimental data are illustrated by symbols: full circles—Yamanaka *et al.* (Ref. 8), triangles—Teraji *et al.* (Ref. 12), open circles—Mortet *et al.* (Ref. 13), and open squares Volpe *et al.* (Ref. 15). (a) The lines show the calculated mobility with $N_A = 10^{16} \text{ cm}^{-3}$ and different compensation densities: $N_D = 0$ —solid line, $N_D = 10^{14} \text{ cm}^{-3}$ —dotted line, $N_D = 10^{15} \text{ cm}^{-3}$ —dashed line, and $N_D = 5 \times 10^{15} \text{ cm}^{-3}$ —dashed-dotted line. (b) The solid lines show the theoretical contribution of various scattering modes and the total mobility (tot) with $N_A = 10^{16} \text{ cm}^{-3}$ and $N_D = 10^{15} \text{ cm}^{-3}$. The scattering mechanisms are ii, ni, ac, and op, calculated respectively from Eqs. (1), (4), (6), and (7).

from 150 to 850 K. The temperature dependence of the four samples are almost the same in the low-temperature range (150–300 K). An unexpected sample-dependent behavior of the mobility is observed at higher temperature (phonon scattering should be intrinsic to diamond and so not sample dependent). Since, the four samples are low boron-doped samples, we assumed for the calculation a low boron density ($N_A = 10^{16} \text{ cm}^{-3}$) which makes negligible the neutral impurity scattering due to neutral boron (ni). For the compensation atom density, we use different values, as shown in Fig. 1(a), ranging between $N_D = 0$ and $N_D = 5 \times 10^{15} \text{ cm}^{-3}$ and giving different ionized impurity scattering contributions to the total mobility. The low-temperature range (below 200 K) is governed by a joined effect of ionized impurity scattering and acoustic phonon scattering. The high-temperature range (larger than 300 K) is dominated by phonon acoustical and optical phonons. Between 200 and 300 K, the mobility is completely limited by acoustical phonon scattering. C_a and $(D_{ii} + D_{ij})$ has been used as adjustable parameters. The best agreement between the experimental data and calculated values is obtained with $C_a = 8.0 \text{ eV}$ and $D_{ii} + D_{ij} = 7 \times 10^9 \text{ eV/cm}$. The coupling constant of the optical phonon scattering is in good agreement with the one determined for natural diamond³⁶ but lower than in homoepitaxial diamond.¹¹ The acoustic deformation potential is found lower than the values determined in the two latter works [14.5 (Ref. 36) and $15.7 \pm 2.6 \text{ eV}$ (Ref. 11)]. It will be shown in the following that the main difference between these works and the present one is the introduction of the neutral impurity scattering in the mobility analysis. The best fit is obtained with $N_D = 10^{15} \text{ cm}^{-3}$ showing that compensation of the four samples is in this range.

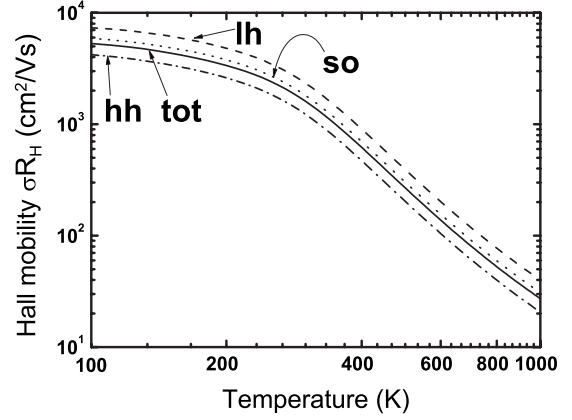


FIG. 2. Temperature dependence of calculated Hall mobility (σR_H) and mobility calculated for the various band taken individually with $N_A = 10^{16} \text{ cm}^{-3}$ and $N_D = 10^{15} \text{ cm}^{-3}$. The solid line is the total mobility (tot), the dashed-dotted for hh band and dotted for so band, and the dashed line for the lh band.

Figure 1(b) shows the various contributions of the scattering mechanisms with $N_A = 10^{16} \text{ cm}^{-3}$ and $N_D = 10^{15} \text{ cm}^{-3}$. As expected for this low doping level, the ni mode is almost negligible in the whole temperature range due to the low density of neutral boron atoms. The ii mode is important between 100 and 200 K due to the ionized compensated centers. Between 200 and 400 K, the ac mode is dominant leading to a power index of the mobility versus T close to $-3/2$. This is in this range that the acoustic deformation potential is determined by comparison with experimental data. Then, the optical phonon branches start to be populate and the op mode controls the high-temperature range of the mobility. It must be noticed that the high-temperature mobility is very large. One gets a value of $100 \text{ cm}^2/\text{Vs}$ at 700 K which is the typical value obtained in 4H-SiC at 300 K.^{17,37}

Figure 2 shows the mobility of the holes in each band calculated individually with $N_A = 10^{16} \text{ cm}^{-3}$ and $N_D = 10^{15} \text{ cm}^{-3}$. As expected, the light holes exhibit the highest mobility of the three band due its lowest effective mass. The spin-orbit holes, which have an effective mass in between light and heavy holes, have a mobility close but slightly higher than the total mobility. The heavy holes is the lowest and the most influencing due to the high density of holes in this band.

B. Mobility in highly boron-doped diamond—temperature dependence

Since the intrinsic parameters due to phonons have been determined in this work, the next step is to study the effect of the impurity scattering which will limit mobility in the low-temperature range (around room temperature in the case of diamond). Figure 3 show the mobility temperature dependence for three boron-doped homoepitaxial diamonds corresponding to samples B37, B42, and B6 of Ref. 11. The boron-doping levels and compensation level of these samples have been determined by the comparison of the hole-density temperature dependence and the neutrality equation (NE) in Ref. 11. It gives $N_A = 2.5 \times 10^{17} \text{ cm}^{-3}$ and $N_D = 10^{15} \text{ cm}^{-3}$

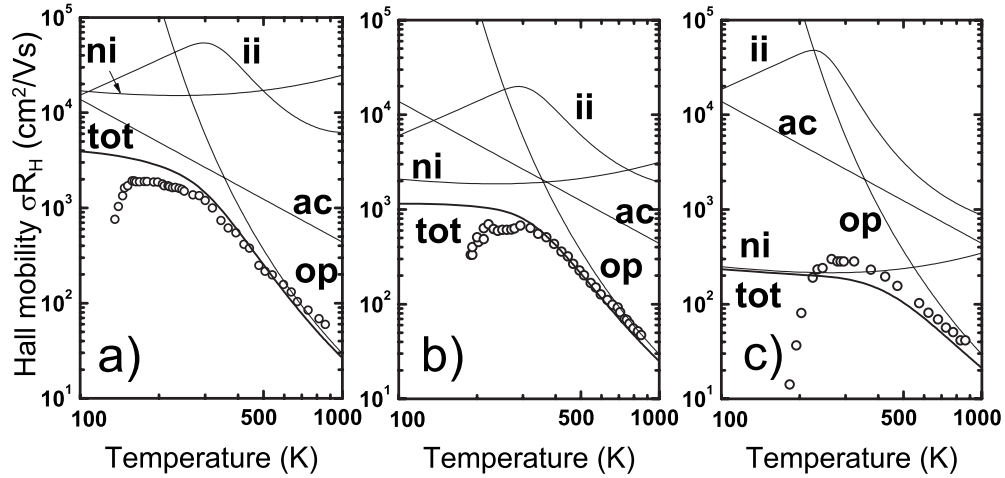


FIG. 3. Temperature dependence of the hole Hall mobility (σR_H) in boron-doped homoepitaxial diamond. (a) Symbols are experimental data of sample B37 from Ref. 11. The solid lines show the theoretical contribution of various scattering modes and the total mobility (tot) with $N_A=2.5 \times 10^{17} \text{ cm}^{-3}$ and $N_D=10^{15} \text{ cm}^{-3}$. (b) Symbols are experimental data of sample B42 from Ref. 11. The solid lines show the theoretical contribution of various scattering modes and the total mobility (tot) with $N_A=2 \times 10^{18} \text{ cm}^{-3}$ and $N_D=3 \times 10^{15} \text{ cm}^{-3}$. (c) Symbols are experimental data of sample B6 from Ref. 11. The solid lines show the theoretical contribution of various scattering modes and the total mobility (tot) with $N_A=1.7 \times 10^{19} \text{ cm}^{-3}$ and $N_D=5 \times 10^{15} \text{ cm}^{-3}$. The scattering mechanisms are ii, ni, ac, and op, calculated respectively from Eqs. (1), (4), (6), and (7).

for sample B37, $N_A=2 \times 10^{18} \text{ cm}^{-3}$ and $N_D=3 \times 10^{15} \text{ cm}^{-3}$ for sample B42, and $N_A=1.7 \times 10^{19} \text{ cm}^{-3}$ and $N_D=5 \times 10^{15} \text{ cm}^{-3}$ for sample B6. The compensation level has been also determined from the fit of the mobility in Ref. 11. A large discrepancy between N_D determined by NE and N_D determined by mobility analysis has been found in the case of the most highly doped samples.

Unfortunately, in this work,¹¹ the neutral impurity has not been introduced in the scattering analysis making the quantitative description of highly doped sample insufficient. In Fig. 3, the mobility temperature dependences of the three samples have been calculated using the same parameters than those determined in the previous section and using impurity parameters determined from the fit of the NE in Ref. 11 given above.

Concerning the B37 sample shown on Fig. 3(a), the low-temperature mobility is controlled mainly by ac mode and the impurity scattering mechanisms (ii and ni) are not important. So, in this case, Tsukioka *et al.*¹¹ found a good agreement between $N_D=1 \times 10^{15} \text{ cm}^{-3}$ by NE fit and $N_D=2 \times 10^{15} \text{ cm}^{-3}$ by mobility fit.

Concerning sample B42, which is ten times more doped than B37, the most important scattering mechanism between 200 and 400 K is the ni mode as shown Fig. 3(b) leading to a mobility near 1000 cm^2/Vs at room temperature. The boron acceptor is quite deep ($E_i \approx 0.37 \text{ eV}$) resulting in an ionization ratio p/N_A lower than few % up to 400 K. This means that the large majority of the boron acceptor are neutral ($N_A=2 \times 10^{18} \text{ cm}^{-3}$ for B42) and then, able to scatter the free holes. Tsukioka *et al.*¹¹ did not take into account the ni mode in the mobility analysis and so overestimated the compensation level in order to increase the influence of the ii mode and by this way, counterbalancing the absence of ni mode to fit the experimental data. That is why the gap between the N_D determined by NE ($3 \times 10^{15} \text{ cm}^{-3}$) is about ten

times lower than the one determined by the mobility analysis ($2.5 \times 10^{16} \text{ cm}^{-3}$).

The effect is huge in the case of sample B6 which is the most highly doped. The low-temperature mobility is completely controlled by ni mode up to 600 K leading to a value close to 200 cm^2/Vs . In this work, the parameters deduced by the NE fit of Tsukioka *et al.*⁸ ($N_A=1.7 \times 10^{19} \text{ cm}^{-3}$ and $N_D=8 \times 10^{14} \text{ cm}^{-3}$) are sufficient to describe the mobility temperature dependence. In their case, for the same reason than for B42 (neglecting the ni mode), they need to overestimate the compensation with $N_D=1.2 \times 10^{19} \text{ cm}^{-3}$ which is more than one hundred times larger than the NE value analysis.

For the three samples, the low-temperature mobility decreases strongly due to a hopping mechanism has already reported in highly boron-doped diamond.^{5,9,38} As expected, the crossing temperature between the hopping regime and the valence-band conduction increases with the boron level [$T(\text{B37})=150 \text{ K}$, $T(\text{B42})=200 \text{ K}$, and $T(\text{B6})=223 \text{ K}$]. For higher temperatures, the agreement between calculation and experimental data is good.

C. Mobility in boron-doped diamond—doping dependence

In this section, the role of the different mechanisms which control the Hall mobility (σR_H) is established as a function of the boron-doping level at 300 and 500 K. In the calculation, the compensation level has been neglected in order to obtain the maximum Hall hole mobility that can be achieved for a given boron-doping level. First, the neutrality equation has been resolved in order to get the density of free holes, ionized impurities, and neutral impurities and to introduce them in the mobility calculation. Then, the mobility values are calculated as a function of the boron density at 300 and 500 K. Figure 4 illustrates the results. At 300 K, the lattice scat-

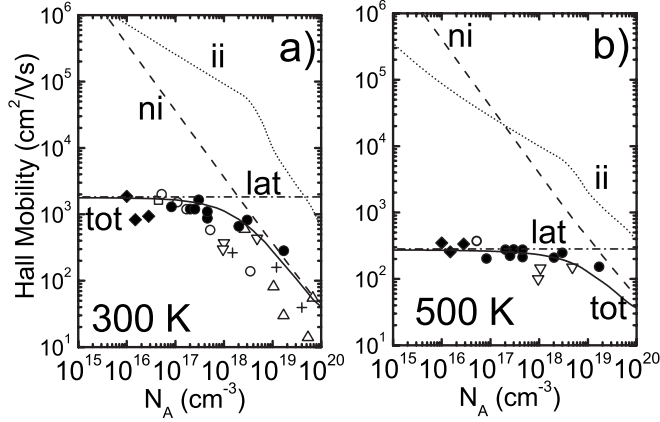


FIG. 4. Hole Hall mobility (σR_H) as a function of doping level in homoepitaxial diamond: (a) at 300 K and (b) at 500 K. The Symbols are experimental data (\blacklozenge —Ref. 15, \bullet —Ref. 11, \square —Ref. 12, \circ —Ref. 13, ∇ —Ref. 14, \triangle —Ref. 7, and $+$ —Ref. 9). The theoretical contribution of various scattering modes are illustrated by dashed and dotted line for lattice (lat=ac+op), dotted line for ii mode and dashed line for ni mode, calculated from Eqs. (1), (4), (6), and (7).

tering (lat=ac+op) is dominant in low-doped materials. The theoretical value of the lattice mobility is $\mu_{lat} \approx 1830$ cm²/Vs. It results from two components which, calculated separately, are: $\mu_{ac} \approx 2660$ cm²/Vs and $\mu_{op} \approx 5850$ cm²/Vs. The mobility is only controlled by the lattice scatterings up to 10^{17} cm⁻³. This intrinsic mobility corresponds to the maximal achievable mobility for *p*-type diamond and is equal to 1830 cm²/Vs. Recent works reported values in this range.^{8,12,13,15} For doping levels above 10^{17} cm⁻³, the ni mode begins to be important. For doping levels above 3×10^{18} cm⁻³, the ni mode is dominant. The ii mode is not important in the whole doping range. This is because: (i) we neglect the compensation and only the ionized boron can scatter the free holes and (ii) the ionization energy of boron is so high than the ratio of ionized boron is small up to high temperature. An increase in the slope is observed in the ii mode for high doping level. This is due to the boron-ionization energy which decreases quickly versus the boron-doping level above 3×10^{18} cm⁻³.³⁹

At 500 K, the phonon branches start to be populated making the lattice scattering mechanisms more important. The theoretical value of the lattice mobility is $\mu_{lat} \approx 280$ cm²/Vs. It results from two components which, calculated separately, are: $\mu_{ac} \approx 1240$ cm²/Vs and $\mu_{op} \approx 360$ cm²/Vs. The mobility is only controlled by the lattice scattering up to 10^{18} cm⁻³. For doping levels above 10^{18} cm⁻³, the ni mode begins to be important. For doping levels above 2×10^{19} cm⁻³, the ni mode is dominant. The ii mode is not important in the whole doping range.

D. Comparison with Si and 4H-SiC

Diamond has a very high hole mobility in comparison to other semiconductors of column IV. Indeed, the hole mobil-

ity in Si and 4H-SiC are close to, respectively, 500 cm²/Vs (Ref. 40) and 100 cm²/Vs (Refs. 17 and 37) in comparison to 1830 cm²/Vs for diamond at 300 K. At 500 K, the hole mobility in Si and 4H-SiC are close to, respectively, 150 cm²/Vs (Ref. 40) and 30 cm²/Vs (Refs. 17 and 37) in comparison to 280 cm²/Vs for diamond. Hole mobility in diamond is also larger than those of electrons in Si and 4H-SiC.^{20,40} The maximum mobility of a semiconductor is governed only by phonons (intrinsic to the material and not impurity or defect dependent). If we simply compare the relevant parameters that appear in acoustical phonon scattering, the diamond mobility is expected to be higher than silicon. Indeed, Eq. (6) shows that the acoustic mode relaxation time is proportional to $\rho v_{||}^2 / (m^{*3/2} C_a^2)$. The acoustical deformation potential C_a is larger in diamond (8 eV) than in silicon (5 eV), the density of states effective mass also ($0.908m_0$ for diamond and $0.81m_0$ for silicon) but the high crystal mass density and the high velocity of the longitudinal acoustic phonons in diamond makes the resulting relaxation time for holes larger in diamond than in silicon. The effective mass of holes in 4H-SiC is so heavy in comparison with diamond or Si that the mobility is significantly lower. The second important reason which makes hole mobility in diamond larger than in silicon is the high optical phonon energy. Even if the coupling constant between hole and optical phonon is high in diamond ($D_{ii} + D_{ij} = 7 \times 10^9$ eV/cm), the optical phonon branches are poorly populated up to a high temperature. The phonon occupation factor $N(\omega_o) = 1 / \{\exp[\hbar\omega_o / (k_B T)] - 1\}$ clearly shows that the high energy of optical phonons in diamond ($\hbar\omega_o = 165$ meV) makes the exponential term very small up to high temperature in comparison with silicon ($\hbar\omega_o = 63$ meV). This also explains the larger mobility of holes in diamond in comparison with electrons in Si and 4H-SiC which have a strong temperature decreasing of the mobility due to optical phonon scattering starting below room temperature as opposite to holes in diamond.

IV. SUMMARY

Hall hole mobility of homoepitaxial boron-doped diamonds has been investigated both theoretically and experimentally. The hole mobility in high-quality diamond has been described in the case of low and high boron-doping levels. It has been shown that the neutral impurity scattering is important in case of strongly doped diamond and limits the mobility for a given boron-doping level. The origin of the superior hole mobility in low doped diamond than in silicon or 4H silicon carbide has been discussed.

ACKNOWLEDGMENTS

This work was financially supported by the Research Program ‘‘Deltadim’’ (Grant No. ANR-BLAN08-3-349825) from French Agence Nationale de la Recherche (ANR) and the Research Programs G.0068.07 and G.0430.07 of the Research Foundation—Flanders (FWO), the Methusalem ‘‘NANO network Antwerp-Hasselt,’’ and the IAP-P6/42 project Quantum Effects in Clusters and Nanowires.

*julien.pernot@grenoble.cnrs.fr

- ¹J. Isberg, J. Hammersberg, E. Johansson, T. Wikström, D. J. Twitchen, A. J. Whitehead, S. E. Coe, and G. A. Scarsbrook, *Science* **297**, 1670 (2002).
- ²M. Nesladek, A. Bogdan, W. Deferme, N. Tranchant, and P. Bergonzo, *Diamond Relat. Mater.* **17**, 1235 (2008).
- ³J. Pernot, C. Tavares, E. Gheeraert, E. Bustarret, M. Katagiri, and S. Koizumi, *Appl. Phys. Lett.* **89**, 122111 (2006).
- ⁴J. Pernot and S. Koizumi, *Appl. Phys. Lett.* **93**, 052105 (2008).
- ⁵T. Klein, P. Achatz, J. Kacmarcik, C. Marcenat, F. Gustafsson, J. Marcus, E. Bustarret, J. Pernot, F. Omnès, B. E. Sernelius, C. Persson, A. Ferreira da Silva, and C. Cytermann, *Phys. Rev. B* **75**, 165313 (2007).
- ⁶E. Bustarret, J. Kačmarčík, C. Marcenat, E. Gheeraert, C. Cytermann, J. Marcus, and T. Klein, *Phys. Rev. Lett.* **93**, 237005 (2004).
- ⁷M. Werner, R. Locher, W. Kohly, D. S. Holmes, S. Klose, and H. J. Fecht, *Diamond Relat. Mater.* **6**, 308 (1997).
- ⁸S. Yamanaka, H. Watanabe, S. Masai, D. Takeuchi, H. Okushi, and K. Kajimura, *Jpn. J. Appl. Phys.* **37**, L1129 (1998).
- ⁹K. Thonke, *Semicond. Sci. Technol.* **18**, S20 (2003).
- ¹⁰C. E. Nebel, *Semicond. Sci. Technol.* **18**, S1 (2003).
- ¹¹K. Tsukioka and H. Okushi, *Jpn. J. Appl. Phys.* **45**, 8571 (2006).
- ¹²T. Teraji, H. Wada, M. Yamamoto, K. Arima, and T. Ito, *Diamond Relat. Mater.* **15**, 602 (2006).
- ¹³V. Mortet, M. Daenen, T. Teraji, A. Lazea, V. Vorliceck, J. D'Haen, K. Haenen, and M. D'Olienslaeger, *Diamond Relat. Mater.* **17**, 1330 (2008).
- ¹⁴M. Gabrysch, S. Majdi, A. Hallén, M. Linnarsson, A. Schöner, D. Twitchen, and J. Isberg, *Phys. Status Solidi A* **205**, 2190 (2008).
- ¹⁵P. N. Volpe, J. Pernot, P. Muret, and F. Omnès, *Appl. Phys. Lett.* **94**, 092102 (2009).
- ¹⁶H. J. Lee and D. C. Look, *J. Appl. Phys.* **54**, 4446 (1983).
- ¹⁷J. Pernot, S. Contreras, and J. Camassel, *J. Appl. Phys.* **98**, 023706 (2005).
- ¹⁸M. Willatzen, M. Cardona, and N. E. Christensen, *Phys. Rev. B* **50**, 18054 (1994).
- ¹⁹*Numerical Data and Functional Relationships in Science and Technology*, Landolt-Börnstein, New Series, Group III Vol. 22, edited by K. H. Hellwege and O. Madelung, Pt. A (Springer, Berlin, 1982).
- ²⁰J. Pernot, W. Zawadzki, S. Contreras, J. L. Robert, E. Neyret, and L. Di Cioccio, *J. Appl. Phys.* **90**, 1869 (2001).
- ²¹J. D. Wiley, in *Semiconductor and Semimetals*, edited by R. K. Willardson and A. C. Beer (Academic, New York, 1975), Vol. 10.
- ²²C. Erginsoy, *Phys. Rev.* **79**, 1013 (1950).
- ²³J. R. Meyer and F. J. Bartoli, *Phys. Rev. B* **24**, 2089 (1981).
- ²⁴L. E. Blagosklonskaya, E. M. Gershenson, Yu. P. Ladyzhinskii, and A. P. Popova, *Fiz. Tverd. Tela (Leningrad)* **11**, 2967 (1969) [*Sov. Phys. Solid State* **11**, 2402 (1970)].
- ²⁵T. C. McGill and R. Baron, *Phys. Rev. B* **11**, 5208 (1975).
- ²⁶E. Gheeraert, A. Deneuveille, and J. Mambou, *Diamond Relat. Mater.* **7**, 1509 (1998).
- ²⁷K. M. Itoh, W. Walukiewicz, H. D. Fuchs, J. W. Beeman, E. E. Haller, J. W. Farmer, and V. I. Ozogin, *Phys. Rev. B* **50**, 16995 (1994).
- ²⁸W. Zawadzki, *Handbook on Semiconductors* (North-Holland, Amsterdam, 1982), Vol. 1, p. 713.
- ²⁹M. Costato, G. Gagliani, C. Jacoboni, and L. Reggiani, *J. Phys. Chem. Solids* **35**, 1605 (1974).
- ³⁰E. M. Conwell and M. O. Vassel, *Phys. Rev.* **166**, 797 (1968).
- ³¹S. A. Solin and A. K. Ramdas, *Phys. Rev. B* **1**, 1687 (1970).
- ³²J. L. Farvacque, *Phys. Rev. B* **62**, 2536 (2000).
- ³³D. C. Look, C. E. Stutz, J. R. Sizelove, and K. R. Evans, *J. Appl. Phys.* **80**, 1913 (1996).
- ³⁴L. Reggiani, D. Waechter, and S. Zukotynski, *Phys. Rev. B* **28**, 3550 (1983).
- ³⁵F. Szmulowicz, *Phys. Rev. B* **28**, 5943 (1983).
- ³⁶K. Tsukioka, *Jpn. J. Appl. Phys.* **40**, 3108 (2001).
- ³⁷A. Koizumi, J. Suda, and T. Kimoto, *J. Appl. Phys.* **106**, 013716 (2009).
- ³⁸T. Sato, K. Ohashi, H. Sugai, T. Sumi, K. Haruna, H. Maeta, N. Matsumoto, and H. Otsuka, *Phys. Rev. B* **61**, 12970 (2000).
- ³⁹J.-P. Lagrange, A. Deneuveille, and E. Gheeraert, *Diamond Relat. Mater.* **7**, 1390 (1998).
- ⁴⁰J. M. Dorkel and Ph. Leturcq, *Solid-State Electron.* **24**, 821 (1981).